sciendo

Polish Journal of Chemical Technology, 21, 4, 106—115, 10.2478/pjct-2019-0046

Prediction of the fixed-bed reactor behavior for biotransformation with parallel enzyme deactivation using dispersion model: A case study on hydrogen peroxide decomposition by commercial catalase

Ireneusz Grubecki[1*], Katarzyna Kazimierska-Drobny[2]

[1]*UTP University of Science and Technology, Department of Chemical and Biochemical Engineering, 3 Seminaryjna Street, 85-326 Bydgoszcz, Poland*

[2]*Kazimierz Wielki University, Department of Mathematics, Physics and Technical Science, 1 Copernicus Street, 85-074 Bydgoszcz, Poland*

[*]*Corresponding author: e-mail: ireneusz.grubecki@utp.edu.pl*

The problems of process costs and pollution of residual waters in the textile industry require increasing attention due to the new ecological regulations and also those resulting from an economic point of view. Hence, the behavior of non-isothermal fixed-bed reactor applied for hydrogen peroxide decomposition by immobilized *Terminox Ultra* catalase attached onto the outer surface of glass beads was studied to determine the operational conditions at which hydrogen peroxide decomposition is most effectively. A dispersion model for bioreactor applied in this work, and verified experimentally, took into account the coupled mass and heat balances as well as the rate equation for parallel enzyme deactivation. The effect of feed temperature, feed flow rate, feed hydrogen peroxide concentration, and diffusional resistances were analysed. In the calculations the global effectiveness factor based on the external mass-transfer model developed previously was employed to properly predict the real bioreactor behavior.

Keywords: Hydrogen peroxide decomposition, Fixed-bed rector, Parallel deactivation, *Terminox Ultra* catalase, Diffusional resistances, Average conversion.

INTRODUCTION

Fixed-bed reactors (FXBR) are important workhorses in biochemical industry because of their efficiency, low cost, and numerous construction, operation, and maintenance advantages. Such reactors are widely employed when the use of immobilized enzymes offers an easy product separation (with less allergenic enzyme impurities), less enzyme loss, increased thermal and operational enzyme stability, enzyme protection against harmful environmental stress, and better control of the process[1]. Thus, design and optimization of such reactors are not an easy task and often involve an inherent trade-off between different conflicting objectives[2]. Especially in case of bioprocesses, optimal conditions assurance can be a very challenging task (even if the process model is available) because of enzyme deactivation which leads to a decrease of the reaction rate and is not always taken into account when predicting proper bioreactor behavior[3]. The factors related to enzyme deactivation characteristics in relationship to the main relation can be decisive in choosing the reactor operating mode[2] and the optimal operating conditions for biotransformations course[4]. Especially, it can be observed in the biotransformations with biocatalyst deactivation dependent on substrate concentration (parallel deactivation). This deactivation mechanism occurs in the case of catalase, which has intensively been applied for elimination of residual hydrogen peroxide (HP) in various domains such as textile, food, semiconductors industries, treatment of the waste waters as well as cosmetics and pharmaceutical formulations in biosensor system[5].

Catalase can be immobilized on the natural and the synthetic carrier materials based on polymers or low molecular compounds, organic or inorganic one[6]. However, when working with the immobilized enzymes (especially catalase), the mass-transfer resistances, i.e. internal and/or external diffusional resistances (IDR/EDR), are likely to occur no matter which method of immobilization is used. It was shown in the hydrogen peroxide decomposition (HPD) by immobilized catalase where transport of substrate through the stagnant layer surrounding the solid biocatalyst particle should not be ignored and the combined effect of EDR and IDR should be taken into account[7].

It is well known that the catalase deactivation rate is high enough at the higher HP concentration, and the use of fixed-bed reactors with immobilized catalase can be inoperable, requiring frequent biocatalyst regeneration/replacement. However, the operational conditions can be pointed out at which the immobilized catalase deactivation rate is not fast. Although, hydrogen peroxide decomposition by catalase has theoretically been studied[8–11] and verified experimentally[12–14], yet in any of these papers the effect of the operating conditions, such as the hydrodynamic conditions, axial dispersion flow, the EDR or/and IDR as well as the rate of enzymatic reaction and biocatalyst deactivation (especially parallel deactivation), on bioreactor behavior have not been considered.

Hence, the objective of the present study was to analyze and simulate the behavior of a non-isothermal fixed-bed reactor performing HPD by a commercial Terminox Ultra Catalase (TUC) immobilized onto the non-porous glass beads at the various operational conditions to determine those at which decomposition process of HP is most effective.

Due to the low HP concentrations occurring in industrial practice, the considerable reaction heat of the enzymatic HPD does not significantly increase the reactor temperature. However, the presented analysis allows us to predict its distribution in the biocatalyst bed in a situation where the HP concentration and/or thermal effect are much higher than those analysed in this study. Moreover,

when the concentration of the enzyme inside the particle is relatively low, the majority of the enzyme should be immobilized at or close to the particle surface[15]. Thus, the use of model solutions showing the reactor behavior can improve the knowledge of the HP decomposed by TUC and the selection of operating conditions for the industrial applications enabling to achieve the maximal bioreactor productivity.

MATHEMATICAL MODEL DEVELOPMENT

Kinetic rate equations for reaction and enzyme deactivation

The rate of changes in the substrate concentration (r_S) of any enzymatic reaction running in the presence of immobilized enzyme can be described by the classical Michaelis-Menten kinetics[16]

$$r_S = \eta_{eff} k'_R(T) \frac{C_E C_S}{(1 + C_S / K_M)} \tag{1}$$

Each biotransformation is accompanied by diminishing activity of biocatalyst the rate of which as a function of substrate concentration[17] and temperature can be expressed as follows

$$r_D = \eta_{eff} k_D \frac{C_E C_S}{(1 + C_S / K_D)} \tag{2}$$

Equation (2) describes the rate of enzyme deactivation dependent on the substrate concentration (parallel deactivation), and particularly can be related to deactivation of catalase by HP.

Bioreactor model

To formulate and then solve the mathematical model of FXBR in which the HPD by immobilized TUC is carried out the following assumptions have been made: 1) catalyst particles are spherical and uniformly packed inside the reactor, 2) the volume and density of the reacting medium are constant, 3) the effective diffusivity does not change throughout the particles and is independent of the HP concentration, 4) the process is diffusion-controlled, 5) the feed and pellets temperatures remain constant, 6) the radial concentration and temperature gradients in the bulk liquid are assumed to be negligible, 7) in industrial practice HPD is carried out at low HP concentration (lower than or equal to 2×10^{-2} kmol · m^{-3}), 8) the substrate (HP) transport rate (r_m) from the bulk liquid (C_S) to the outer surface of the immobilized bead (C_{SS}) is controlled by equimolar diffusion described by Eq. (3)

$$r_m = k_{mL} a_m (C_s - C_{ss}) \tag{3}$$

Mass and energy balances with enzyme deactivation rate equation

Accounting for the above assumptions and introducing dimensionless state variables

$$\overline{C}_E = \frac{C_E}{C_{E0}}, \quad \overline{C}_S = \frac{C_S}{C_{S,In}}, \quad \vartheta = \frac{T}{T_{In}} \tag{4}$$

a dimensionless axial coordinate variable (h) and a dimensionless biocatalyst age (τ)

$$h = \frac{z}{L}, \quad \tau = t \frac{U_S}{L} \tag{5}$$

as well as the dimensionless process parameters

$$\mathrm{Pe}_{mL} = \frac{U_S L}{\varepsilon D_L}, \quad \mathrm{Pe}_{qL} = \frac{\rho C_P U_S L}{\varepsilon \Lambda_x}, \quad \mathrm{St}_H = \frac{4\alpha_W}{D_R \rho C_P} \frac{L}{U_S} \tag{6a}$$

$$\mathrm{K}_1 = k_R a_m \frac{L}{U_S}, \qquad \mathrm{K}_2 = k_D C_{S,In} \frac{L}{U_S} \tag{6b}$$

$$\mathrm{H}_R = \frac{(-\Delta H_R) C_{S,In}}{\rho C_P T_{In}}, \quad \beta_i = \frac{E_i}{R T_{In}} \quad (i = \mathrm{D}, \mathrm{R}) \tag{6c}$$

the mathematical expressions of the mass and energy balances in the bulk liquid phase as well as an equation for the enzyme deactivation rate describing the course of HPD process in fixed-bed bioreactor with external heat exchange can be written in form of Eqs. (7)–(9)

$$\varepsilon \frac{\partial \overline{C}_S}{\partial \tau} = \mathrm{Pe}_{mL}^{-1} \frac{\partial^2 \overline{C}_S}{\partial h^2} - \frac{\partial \overline{C}_S}{\partial h} - \eta_{eff}(1-\varepsilon)\mathrm{K}_1 \overline{C}_E \overline{C}_S \tag{7}$$

$$\varepsilon \frac{\partial \vartheta}{\partial \tau} = \mathrm{Pe}_{qL}^{-1} \frac{\partial^2 \vartheta}{\partial h^2} - \frac{\partial \vartheta}{\partial h} + \mathrm{St}_H(\vartheta_W - \vartheta) - \eta_{eff}(1-\varepsilon)\mathrm{K}_1 \mathrm{H} \overline{C}_E \overline{C}_S \tag{8}$$

$$-\frac{\partial \overline{C}_E}{\partial \tau} = \eta_{eff}(1-\varepsilon)\mathrm{K}_2 \overline{C}_E \overline{C}_S \tag{9}$$

The initial ($\tau = 0$) and boundary conditions for Eqs. (7)–(9) at the entry ($h = 0$) and the exit ($h = 1$) from bioreactor are given by

$$\tau = 0, \qquad 0 \le h \le 1: \qquad \overline{C}_S = \overline{C}_E = \vartheta = 1 \tag{10}$$

$$\tau > 0, \qquad h = 0: \qquad \mathrm{Pe}_{mL}^{-1} \frac{\partial \overline{C}_S}{\partial h} = \overline{C}_S - 1, \tag{11}$$

$$\mathrm{Pe}_{qL}^{-1} \frac{\partial \vartheta}{\partial h} = \vartheta - 1$$

$$\tau > 0, \qquad h = 1: \qquad \frac{\partial \overline{C}_S}{\partial h} = \frac{\partial \vartheta}{\partial h} = 0 \tag{12}$$

The term of $\mathrm{St}_H(\vartheta_W - \vartheta)$ describing the heat transfer between the bioreactor wall and the bulk liquid phase has been introduced into Eq. (8) due to assumed one--dimensional model.

The formulated mathematical model allows to predict the real behavior of the fixed-bed bioreactor for HPD process occurring in the presence of a commercial catalase applied in industrial practice.

Evaluation of the effectiveness factor

It was proved[7] that in the HPD process occurring in the presence of immobilized TUC the EDR should not be neglected (Table 1).

Then, to properly assess the real bioreactor behavior, the global effectiveness factor appearing in Eqs. (1), (2) and (7)–(9) should be introduced[2]

$$\eta_{eff} = \frac{\mathrm{Bi}[\tanh^{-1}(3\phi) - (3\phi)^{-1}]}{\phi[\mathrm{Bi} - 1 + 3\phi \tanh^{-1}(3\phi)]} \tag{13}$$

where Bi ($=k_{mL} d_P / 6 D_{eff}$), and φ ($=d_P/6(k_R a_m / D_{eff})^{0.5}$) represent the Biot number and Thiele modulus for biochemical reaction of first-order kinetics, respectively, and calculated using external mass-transfer model developed previously[7] as well as the kinetic parameters for

Table 1. The value of Biot number, Bi, estimated at different values of feed flow rate, Q, as well as for lower T_{min} and upper T_{max} temperature constraints

$Q\times10^8$	T_{min} = 293K		T_{max} = 323K	
$m^3\cdot s^{-1}$	Bi	ϕ	Bi	ϕ
166.7	31.1		29.4	
125.0	25.9		24.5	
83.3	20.1		19.0	
41.7	13.0		12.2	
25.0	9.38	2.590	8.86	2.314
16.7	7.26		6.86	
8.33	4.68		4.43	
3.33	2.62		2.48	
1.67	1.69		1.60	

For $Q\times10^8 \geq 25$ $m^3\cdot s^{-1}$ the EDR are non-significant and rate of HPD can be controlled by IDR slightly decreasing with temperature ($\eta_{IDR} = 0.33$ for T_{min} = 293K and $\eta_{IDR} = 0.37$ for T_{max} = 323K). On the contrary, when $Q\times10^8 < 25$ $m^3\cdot s^{-1}$ the combined effect of EDR and IDR appears.

reaction and deactivation describing the process free of diffusional resistances. The behavior of the effectiveness factors under EDR, and the combined effect of EDR and IDR (Eq. (13)) have been depicted on Fig. 1.

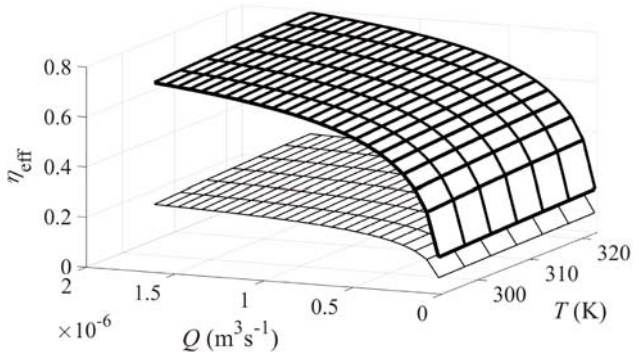

Figure 1. Effectiveness factor η_{eff} under EDR, $\eta_{eff} = \eta_{EDR}$, (upper surface), as well as combined effect of EDR and IDR, $\eta_{eff} = \eta_G$, (lower surface) as a function of feed flow rate (Q) and temperature (T)

Calculation of effective diffusion coefficient

To represent the role of porosity on diffusion, free diffusivity in a fluid without obstacles must be scaled with tortuosity, i.e. the diffusion path of species accounting for the deviation from straight line. In this paper, the frequently used tortuosity-porosity relation[18] was applied to estimate the effective diffusivity

$$D_{eff} = D_f \frac{\varepsilon_P}{\tau} \tag{14}$$

where τ is tortuosity factor expressed as follows[19]

$$\tau^2 = \frac{\varepsilon_P}{1-(1-\varepsilon_P)^{1/3}} \tag{15}$$

and ε_P is the effective, transport-through porosity of the considered structure assumed to be 0.5[20].

Criteria for bioreactor performance

Time-average HP conversion

Conversion is a convenient variable and is often used instead of concentration in engineering work. Hence, to assess the reaction progress, and consequently, bioreactor performance the time-average substrate conversion obtained from the solution of the convection-diffusion--reaction equations has been introduced.

$$\alpha_m = \frac{1}{\tau_f}\int_0^{\tau_f}[1-C_S(h,\tau)/C_{S,In}]\,d\tau \tag{16}$$

Distribution of biocatalyst activity

Distribution of biocatalyst activity allows to indicate the moment in which an enzyme catalyst must be discarded and replaced. It is a major issue in biotransformations being a crucial decision in process economics, at the same time.

MATERIAL AND METHODS

Enzyme immobilization

Terminox Ultra catalase (E.C. 1.11.1.6; 50,000 U · g^{-1}) was covalently immobilized onto non-porous glass beads modified with 3-aminopropyltriethoxysilane followed by a treatment with glutaraldehyde as it was described in the previous report[7]. Glass beads, glutaraldehyde (50% (w/w) aqueous solution) as well as 3-aminopropyltriethoxysilane were purchased from Sigma-Aldrich (Steinheim, Germany). All the other chemical reagents of analytical grade, including commercial hydrogen peroxide (30% (w/w) aqueous solution), were products of Avantor Performance Materials (Gliwice, Poland).

Packed-bed reactor studies

Apparatus

Three glass columns with a jacket of water recirculation were each filled with identical 11 g of immobilized TUC established earlier. These three reactors were combined in series with provisions for taking an effluent sample from each of them. Thus, this system may be considered as a single long packed-bed reactor (Table 2) enabling controlling substrate (especially HP) conversion as a function of biocatalyst age t ($\tau = tQ\varrho_U/W$), and reactor position z ($h = z/L$). More details can be found in the study presented previously[7]. The feed solution with HP concentration of $C_{S,In} = 5\times10^{-3}$ kmol · m^{-3} was pumped through the bed by a peristaltic pump (Model 7518-00, Cole Parmer Ltd., USA) at the fixed volumetric flow Q ranging from 166.7×10^{-8} $m^3 \cdot s^{-1}$ to 1.67×10^{-8} $m^3 \cdot s^{-1}$ and controlled by a flowmeter.

Table 2. Characteristics of the model reactor and biocatalyst employed in calculations

Reactor sizes	
Length (m)	0.36
Diameter ($\times10^{-3}$ m)	8.00
Cross section ($\times10^{-5}$ m^2)	5.03
Total volume ($\times10^{-5}$ m^3)	1.81
External surface/reactor volume unity ($\times10^3$ m^{-1})	8.32
Bed characteristics	
Particle diameter ($\times10^{-4}$ m)	5.05
Bed density ($\times10^3$ kg m^{-3})	1.82
Total biocatalyst weight in reactor ($\times10^{-3}$ kg)	33.0
Total biocatalyst volume in reactor ($\times10^{-6}$ m^3)	12.67
Free volume ($\times10^{-3}$ m^3)	5.43
Porosity	0.30

Estimation of intrinsic kinetic constants for reaction and enzyme deactivation

The intrinsic rate constants for reaction (k_R) and deactivation (k_D) were determined according to the method described previously[7] yielding the activation energies and frequency factors for reaction and deactivation, respectively, to be E_R = 12.6 ± 0.3 kJ mol^{-1}, and $k_{R0}a_m$ = 48.00 ± 5.38 s^{-1} as well as E_D = 49.7 ±1.2 kJ mol^{-1}, and k_{D0} = (2.77 ± 1.08) × 10^7 m^3 · kmol^{-1} · s^{-1}. These kinetic parameters of the immobilized TUC represent its proper behaviour when the external diffusional restrictions can be disregarded. Such conditions (feed flow rate) have been established by monitoring the HP concentration at the outlet stream under the various feed flow rates, Q, and invariable residence time.

Correlations for the dispersion coefficients

Péclet number from exit age distribution

The method based on measuring the longitudinal spreading of the tracer concentration (C_S) in the exit stream as a function of time (t) was employed, enabling to estimate a value of the Péclet number (Pe_{mL}), and hence, a value of the dispersion coefficient D_L. A solution of hydrogen peroxide with concentration of 7.8×10^{-2} kmol · m^{-3} was used as a tracer. After a steady liquid flow was attained, 1×10^{-3} m^3 of the tracer was quickly injected. The tracer injection time was kept as low as possible, so as to achieve almost ideal pulse input conditions. The response (HP concentration vs. time) for the reactor outlet was spectrophotometrically monitored. The relationship between the variance of the concentration versus the dimensionless time ($\theta = t/t_m$) curve and the Péclet number (Pe_{mL}) for a closed-closed system can be expressed by[21]

$$\sigma_\theta^2 = \frac{\sigma_t^2}{t_m^2} = \frac{2}{Pe_{mL}}\left[1 - \frac{1-\exp(-Pe_{mL})}{Pe_{mL}}\right] \quad (17)$$

Based on the response curve, the values of the mean residence time t_m and variance σ_t^2 were assessed to calculate Pe_{mL} for each analysed feed flow rate. In consequence, a dependence Pe_{mL} vs. Re was developed to be

$$Pe_{mL} = 0.484Re + 1.420 \quad (18)$$

The developed model (Eq. (18)) offers quite a good fit to the experimental data, and can successfully be applied to properly predict the bioreactor behavior (the model equations (7)–(12)).

The longitudinal thermal dispersion coefficient

The experimental correlation describing the effect of Reynolds (Re) and Prandtl (Pr) numbers on the thermal dispersion coefficient (Λ_x) and developed by Testu et al.[22] was used in calculations

$$\Lambda_x = 1.3 + 0.607\varepsilon(1-\varepsilon)\,Re^{1.5}\left[\frac{8.87(Pr-0.7) - 0.543\,(Pr-7.02)}{6.32}\right] \quad (19)$$

Equation (19) is applicable for a water/glass and air/glass beads systems in the 0 < R ≤ 130 range.

Determination of hydrogen peroxide concentration

The concentration of HP in the feed and effluent streams of the reactor was monitored spectrophotometrically making use of a UV-Vis Jasco V-530 spectrophotometer (Artisan T.G., Champaign IL, USA) equipped with a quartz cuvette Q11020 (Gallab, Warsaw, Poland) with optical light path of 20 mm, until the tracer concentration was reduced to near zero. The measurements were carried out at 240 nm (ε_{240} = 39.4 dm^3 · mol^{-1} · cm^{-1}).

RESULTS AND DISCUSSION

There are many parameters that significantly influence the HPD in the presence of immobilized TUC. In industrial practice, the most important parameters are the feed temperature, T_{In}, the feed HP concentration, $C_{S,In}$, as well as the feed flow rate, Q, corresponding to diffusional resistances expressed by the effectiveness factor, η_{eff}. Hence, the performance of a non-isothermal tubular reactor packed with spherical enzyme particles has been modeled in terms of these parameters. The formulated mathematical model described by Eqs. (4)–(12) with Eqs. (13)–(15), (18) and (19) has been solved with MATLAB using Partial Differential Equations Toolbox (Mathworks Inc., Natick MA, USA).

Hydrogen peroxide conversions obtained during kinetics assays in the model reactor (Table 1) with TUC immobilized on non-porous beads as a function of the biocatalyst ages (t), feed flow rate (Q), and axial positions (h) have been shown in Figs. 2(a) and 2(b). Moreover, the theoretical values represented by the solid lines were predicted using the same experimental conditions. In this analysis, the lower and the upper temperature constraints equal to T_{min} = 293K and T_{max} = 323K, respectively, have been taken into account owing to the optimal operational activity of *Terminox Ultra* catalase[4].

As it can be observed (Fig. 2(a)), the lower feed flow rates, Q, the higher HP conversion can be obtained. Furthermore, for the feed flow rate Q of 5×10^{-8} m^3 · s^{-1} and biocatalyst age of t_f = 16 h, HP conversion values higher than 92% and 99% were obtained after attaining 1/3 and 2/3 of the total bioreactor length, respectively, while these values reached approximately 87% and 97%, for 10×10^{-8} m^3 · s^{-1} as well as 71% and 93% for 20×10^{-8} m^3 · s^{-1}, respectively. In view of the results presented in Figs. 2(a) and 2(b) it can be stated that the theoretical model expressed by (Eqs. (4)–(15)) predicts the experimental behavior with a smaller error, less than 3.0%.

It has been mentioned that assurance of the optimal strategy in FXBR for decomposition process of HP can be a very challenging task. However, such an operating strategy can be simply accomplished by searching for a suitable feed temperature that under a constant feed flow rate yields the maximum bioreactor productivity. Thus, bearing in mind good consistency of the experimental data with those obtained as a result of theoretical prediction, the analysis was performed to search for a suitable feed temperature yielding the maximum value of the time-average HP conversion at the reactor outlet, and providing a compromise between the rate of reaction and that of enzyme deactivation. This feed temperature was obtained using a constrained non-linear minimization with MATLAB Optimization Toolbox (Mathworks

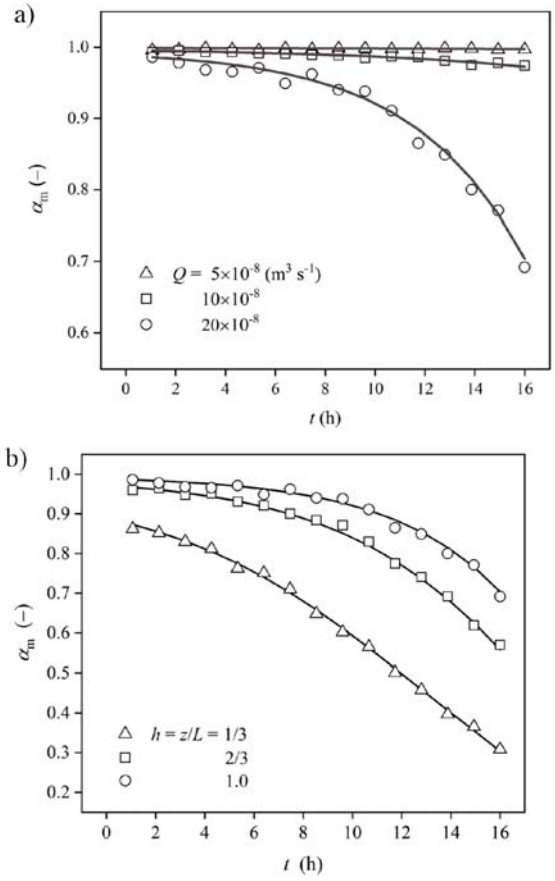

Figure 2. Theoretical prediction (solid lines) and experimental data (open symbols) for HP conversion obtained in the process under EDR for $C_{S,In} = 5 \cdot 10^{-3}$ kmol m^{-3}: (a) at the reactor outlet (h = 1) for different feed flow rates (Q), (b) for $Q = 20 \cdot 10^{-8}$ m^3 s^{-1} and various axial positions (h) in the bioreactor

Inc., Natick MA, USA). In the optimization procedure, the MATLAB Partial Differential Equation Toolbox was employed to solve the set of non-linear partial differential equations (Eqs. (7)-(9)). The calculations were performed for the reaction heat of HPD equal to $(-\Delta H_R) = 93$ kJ · mol^{-1} [23] as well as for the coefficient of heat transfer between wall and bulk liquid phase $\alpha_W = 330$ W · m^{-2} · K^{-1}, and calculated according to the correlation of Dixona and Cresswell[24].

Moreover, the EDR assessment is crucial to properly predict the behavior of the fixed-bed reactor. Hence, it was proved that in the HPD process occurring in the presence of immobilized catalase the EDR should not be neglected compared to IDR[7]. Thus, in this analysis the effect of EDR as well as combined effect of EDR and IDR have been taken into account.

As noted, the decomposition process of HP in industrial practice progresses in the range of low HP concentrations $C_{S,In}$ (lower or equal to 2×10^{-2} kmol · m^{-3}). Thus, figures 3(a) and 3(b) depict the effect of the feed temperature (T_{In}) and the volumetric flux (Q) on the time-average substrate conversion at the reactor outlet for the feed HP concentration of $C_{S,In} = 5\times10^{-3}$ kmol · m^{-3}. Variations of ($Q\times10^8$) ranging from 20 m^3 · s^{-1} to 1.67 m^3 · s^{-1} cause a decrease of the effectiveness factors from 0.456 to 0.163 for the HPD under EDR as well as from 0.188 to 0.074 for the process under the combined effect of EDR and IDR, respectively.

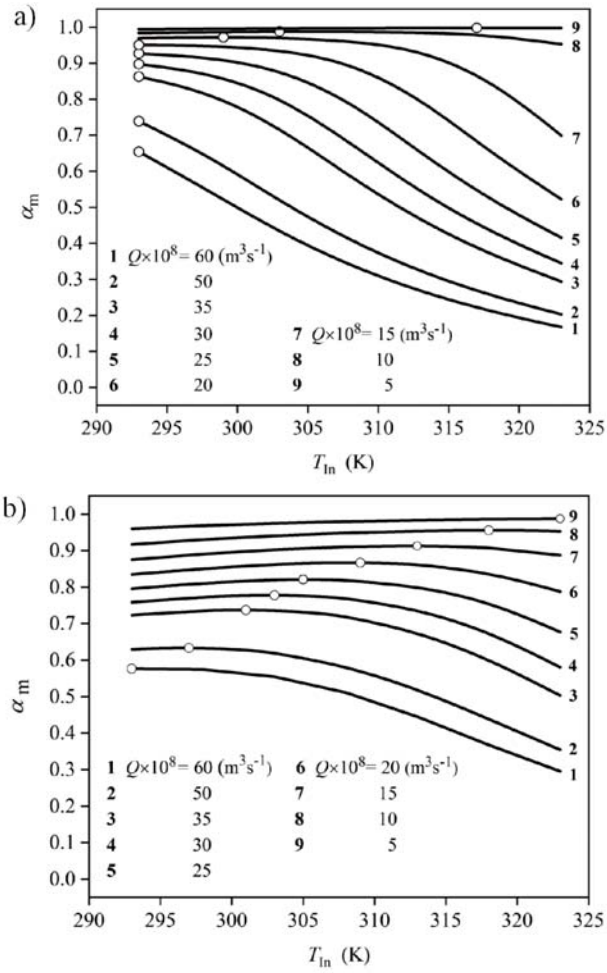

Figure 3. Effect of feed temperature T_{In} and feed flow rate, Q, on time-average HP conversion in the process under: a) EDR, b) combined effect of EDR and IDR occurring in FXBR with heat exchanger for $\vartheta_W = 1$, and $C_{S,In} = 5 \cdot 10^{-3}$ kmol m^{-3}. Open symbols represent the maximum (or the highest)

It can be said that for the analyzed values of the kinetic and mass-transfer parameters such a feed temperature can be indicated, that maximizes the time-averaged HP conversion at the reactor outlet. This feed temperature (say optimal feed temperature, OFT) exists only for a certain value (at least one) of the feed flow rate $Q^\bullet$ (corresponding to the effectiveness factor $\eta_{eff}^\bullet$). For the feed flow rates higher than $Q^\bullet$ ($Q > Q^\bullet$), the average HP conversion decreases with raising temperature, and then the OFT becomes equal to the lower temperature constraint, T_{min}. On the contrary, for the feed flow rates lower than $Q^\bullet$ ($Q < Q^\bullet$), the average HP conversion increases with the raising temperature, and the OFT should be equal to the upper allowable temperature, T_{max}. Thus, there exists such a feed temperature value for which the time-average HP conversion is maximal (Figs. 3(a), lines 7–9, and 3(b), lines 2–8). The more significant diffusional resistances, the higher the OFT ensuring the time-average maximum HP conversion is.

Distributions of the HP concentration $\overline{C}_S(h,\tau)$, and TUC activity $\overline{C}_E(h,\tau)$ calculated for $Q = 20\times10^{-8}$ m^3 · s^{-1} and corresponding to the OFT equal to 293K for the HPD process under EDR, and 308K for the process under combined effect of EDR and IDR, have been shown on Figs. 4 and 5. Due to the clarity of the

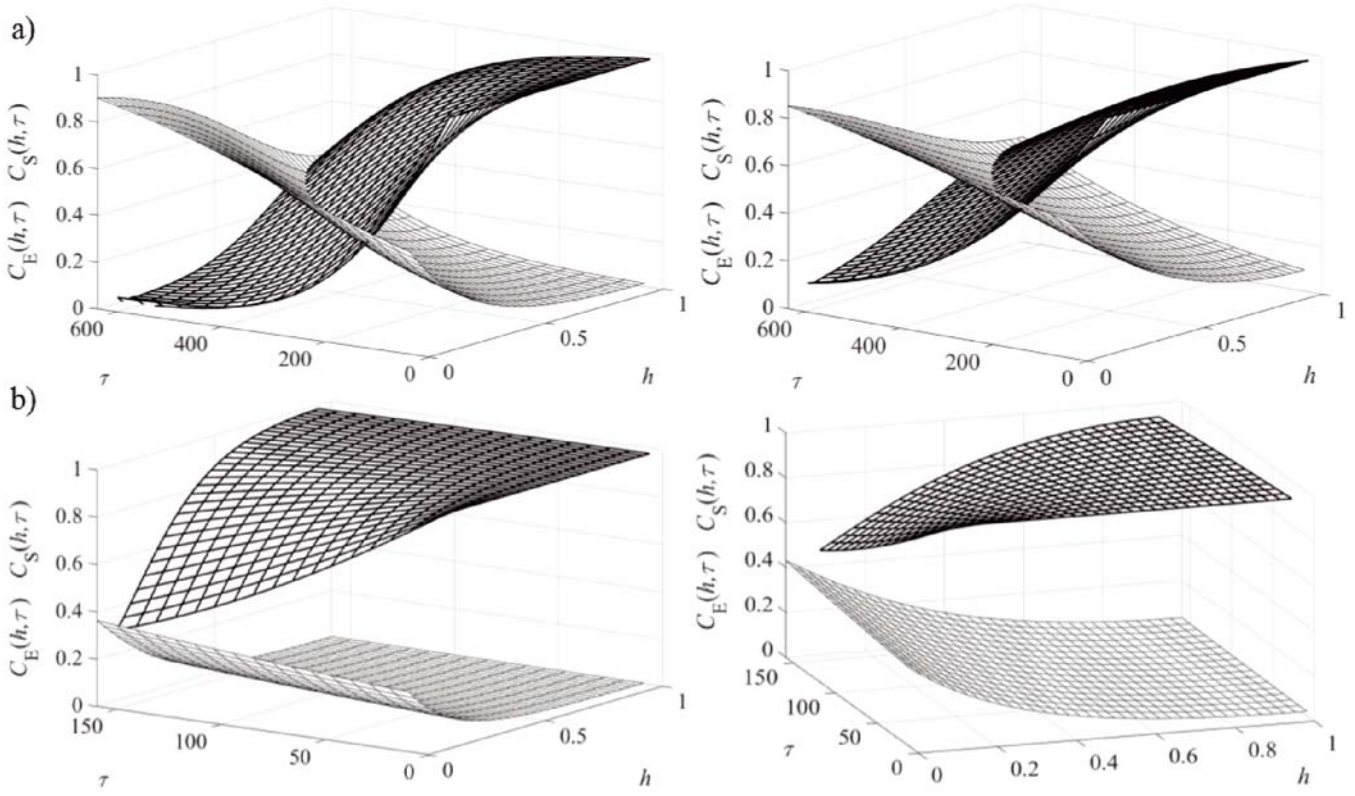

Figure 4. Distributions of HP concentration $\overline{C}_S(h,\tau)$ (lower surface), and TUC activity $\overline{C}_S(h,\tau)$ (upper surface) in the HPD process under EDR (left), as well as under combined effect of EDR and IDR (right) for $C_{S,In} = 5 \cdot 10^{-3}$ kmol $\cdot$ m^{-3}, and various feed flow rates: (a) $Q = 20 \cdot 10^{-8}$ m$^3 \cdot$ s^{-1}, $\tau_f = 640$, (b) $Q = 5 \cdot 10^{-8}$ m$^3 \cdot$ s^{-1}, $\tau_f = 160$. Calculations have been made for OFT of 308 K ($\vartheta_W = 1$)

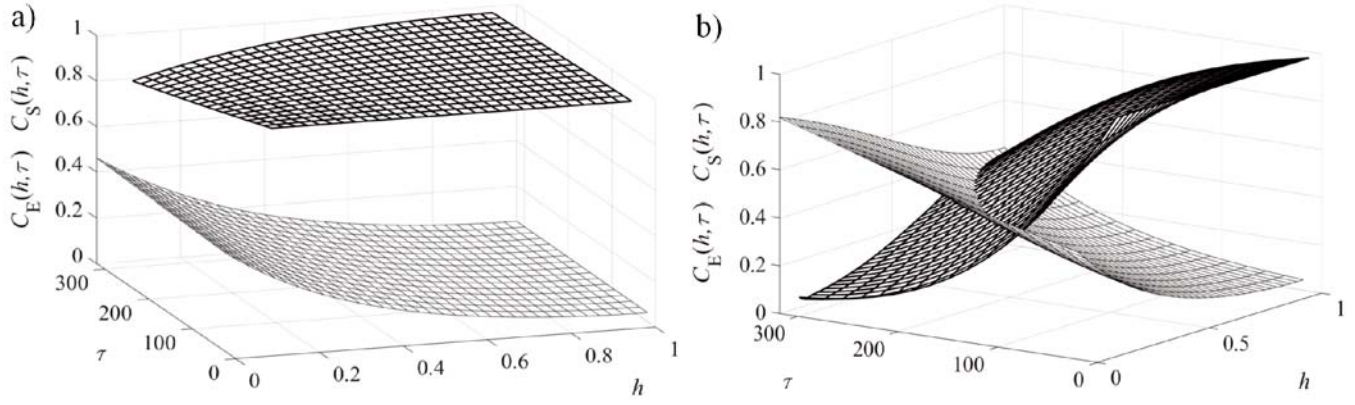

Figure 5. Distributions of HP concentration $\overline{C}_S(h,\tau)$ (lower surface) and TUC activity $\overline{C}_E(h,\tau)$ (upper surface) as a functions of dimensionless bioreactor length (h) and biocatalyst age (τ) in the HPD process under combined effect of EDR and IDR, for feed flow rate of $Q = 10 \cdot 10^{-8}$ m$^3 \cdot$ s^{-1}, and feed concentrations equal to: a) $1 \cdot 10^{-3}$ kmol $\cdot$ m^{-3}, b) $1 \cdot 10^{-2}$ kmol $\cdot$ m^{-3}. Calculations have been made for OFT of 308 K ($\varrho_W = 1$)

mentioned figures the calculation results for the first step have been disregarded.

In general, it can be observed that in the biotransformations with parallel enzyme deactivation the biocatalyst activity distribution, $\overline{C}_E(h,\tau)$, is the reflection the changes of substrate concentration, $\overline{C}_S(h,\tau)$. The high biocatalyst activity results in the fast HP decomposition. In effect, the low HP concentration leads to slow TUC deactivation. Thus, the highest HP conversion (the lowest TUC activity) is achieved only during the initial run of the bioreactor. Furthermore, the lower the feed HP concentration, and the shorter the biocatalyst age, the higher the HP conversion can be obtained (Table 3).

Table 3. Exemplary values of average HP conversion, α_m, at the reactor outlet for various feed HP concentration, and biocatalyst ages, τ_f

	τ_f					
$C_{S,In} \times 10^3$	265		530		795	
kmol $\cdot$ m^{-3}	EDR	G	EDR	G	EDR	G
1	0.955	0.881	0.953	0.874	0.950	0.866
5	0.942	0.847	0.886	0.772	0.701	0.650
10	0.886	0.771	0.520	0.515	0.342	0.340
15	0.670	0.649	0.341	0.340	0.218	0.216

EDR – process under external diffusional resistance, G – process under combined effect of EDR and IDR

Additionally, the lower the feed flow rate, the higher the time-average HP conversion can be expected (Fig. 5). The last regularity is the reason for which in the HPD occurring in the presence of TUC undergoing deactivation the operating strategy should be accomplished in such a way that the feed flow rate decreases with time to compensate the loss of enzyme activity. The lower the feed flow rate, the more significant EDR (at the same time combined effect of EDR and IDR), and then the slower the biocatalyst deactivation should be expected. Consequently, the higher time-average values of HP conversion at the reactor outlet, and biocatalyst activity in the bed are required. For example, in the HPD process occurring under EDR, the time-average HP conversion, α_m, and TUC activity, $\overline{C}_{Em}(\tau=\tau_f,h)$, are equal to 0.884 and 0.159, respectively, for $Q = 25\times10^{-8}$ $m^3\cdot s^{-1}$, 0.938 and 0.286 for $Q = 20\times10^{-8}$ $m^3\cdot s^{-1}$, 0.970 and 0.445 for $Q = 15\times10^{-8}$ $m^3\cdot s^{-1}$, 0.988 and 0.621 for 10×10^{-8} $m^3\cdot s^{-1}$, as well as 0.997 and 0.804 for 5×10^{-8} $m^3\cdot s^{-1}$. While in the process under combined effect of EDR and IDR the mentioned values of the time-average HP conversion and average TUC activity in the bed are assumed to be 0.746 and 0.289, respectively, for $Q = 25\times10^{-8}$ $m^3\cdot s^{-1}$, 0.812 and 0.380 for $Q = 20\times10^{-8}$ $m^3\cdot s^{-1}$, 0.874 and 0.498 for $Q = 15\times10^{-8}$ $m^3\cdot s^{-1}$, 0.928 and 0.673 for 10×10^{-8} $m^3\cdot s^{-1}$, as well as 0.972 and 0.809 for 5×10^{-8} $m^3\cdot s^{-1}$. It is then obvious that the greater the distance from the reactor inlet, h, the lower the HP concentration is. Consequently, biocatalyst activity grows when, h, increases.

When the effect of external film diffusion can be disregarded then the process course is controlled by IDR related to the mass-transport of HP inside the pores of the support. Figure 6 shows the dependence illustrating the influence of effectiveness factor under IDR, η_{IDR}, and the feed flow rate, Q, on OFT. Due to clarity of Fig. 6, the relationship $T_{In,opt}$ vs η_{IDR} has been presented only for the selected values of $Q\times10^8$ (= 5, 10, 20, 25 $m^3\cdot s^{-1}$), for which the differences in the curve courses are substantial.

Generally, in a situation when EDR can be negligible (similarly when the combined effect of EDR and IDR appears), for any value of Q, a certain values of $\eta^{\bullet}_{IDR}$ can be indicated that at $\eta_{IDR} > \eta^{\bullet}_{IDR}$, the OFT is equal to T_{min} ($T_{In,opt} = T_{min}$), while at $\eta_{IDR} < \eta^{\bullet}_{IDR}$, $T_{In,opt} = T_{max}$. Flow slowdown gives rise to a shift of the $\eta^{\bullet}_{IDR}$ values toward the higher values. Especially, for the HPD process, the value of $\eta_{IDR} = 0.354$ has been assumed for the kinetic and mass-transfer parameters considered in this work and calculated for a moderate temperature of 303K. It can be seen that when in the HPD process the biocatalyst is applied for which $\eta_{IDR} = 0.354$, the OFT maximizing the time-average HP conversion at the reactor outlet corresponds to the lower allowable temperature equal to $T_{min} = 293$ K. Then, the average HP conversion, and TUC activity in the bed are assumed to be 0.872 and 0.495, respectively, for $Q = 25\times10^{-8}$ $m^3\cdot s^{-1}$, 0.916 and 0.575 for $Q = 20\times10^{-8}$ $m^3\cdot s^{-1}$, 0.954 and 0.666 for $Q = 15\times10^{-8}$ $m^3\cdot s^{-1}$, 0.982 and 0.768 for 10×10^{-8} $m^3\cdot s^{-1}$, as well as 0.997 and 0.878 for 5×10^{-8} $m^3\cdot s^{-1}$. It should be noted that the predicted values of HP conversion for the HPD process under IDR take the values between those calculated for the process under EDR, and the combined effect of EDR and IDR, while the average TUC activity in the bed – due to the lower value of OFT (less significant diffusional resistances) – is the higher.

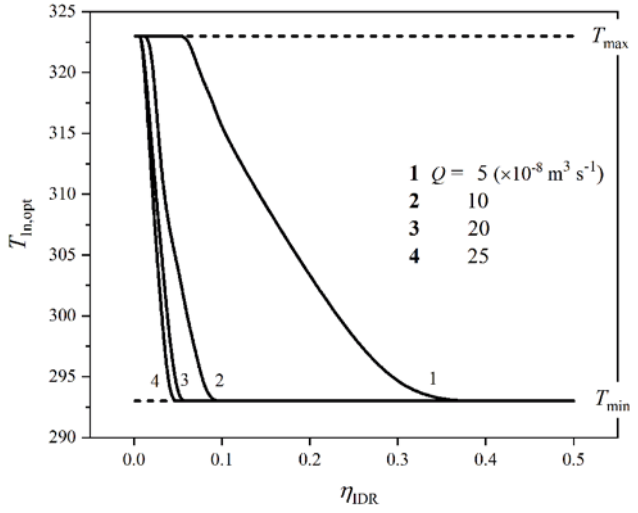

Figure 6. Effect of effectiveness factor under IDR, η_{IDR}, and feed flow rate, Q, on OFT, $T_{In,opt}$, ensuring the maximum time-average outlet HP conversion, α_m

The use of biocatalyst of η_{IDR} value lower than 0.354 increases the OFT (Fig. 6) yielding the lower HP conversions, and consequently, the higher biocatalyst activity in the bed.

Inclusion the energy balance equation (Eq. (8)) in the mathematical model allows predicting the temperature conditions existing in bulk of the liquid phase. It has been mentioned that in industrial applications the HPD process runs at the HP concentrations lower than 2×10^{-2} $kmol\cdot m^{-3}$. Such a low concentration makes the temperature rise along the length of bioreactor negligible so the temperature conditions in the reactor can be considered as isothermal. On the other hand, more detailed analysis showed that the temperature distribution in the bed, $\vartheta(h,\tau)$, is independent of the reaction heat. What does change is the value of the maximum temperature reached in the reactor and at higher substrate concentration it may be higher by a few to even dozen or so degrees in comparison with the feed temperature, T_{In}. The occurrence of the maximum temperature is mostly dependent on the feed flow rate, and the feed HP concentration (see Figs. 7(a) and 7(b)). The higher the feed HP concentration, the faster TUC deactivation arises. As a result, the most significant temperature growth compensating the loss of TUC activity can be expected in the initial part of the bioreactor, while the higher the feed HP concentration, the more rapid temperature increase is, with a maximum appearing closer to the reactor inlet. Additionally, the lower the feed flow rate, the temperature maximum more pronounced is. These regularities can be particularly useful in determining the optimal feed temperature, which provides the maximum performance of the reactor[25].

The described temperature variations appear when the feed temperature equals to that of the jacket fluid and correspond to the general regularities which reveal when the biotransformations with biocatalyst deactivation, especially parallel deactivation occur. It is worth to mention that the bulk liquid temperature under the considered values of the kinetic and transport parame-

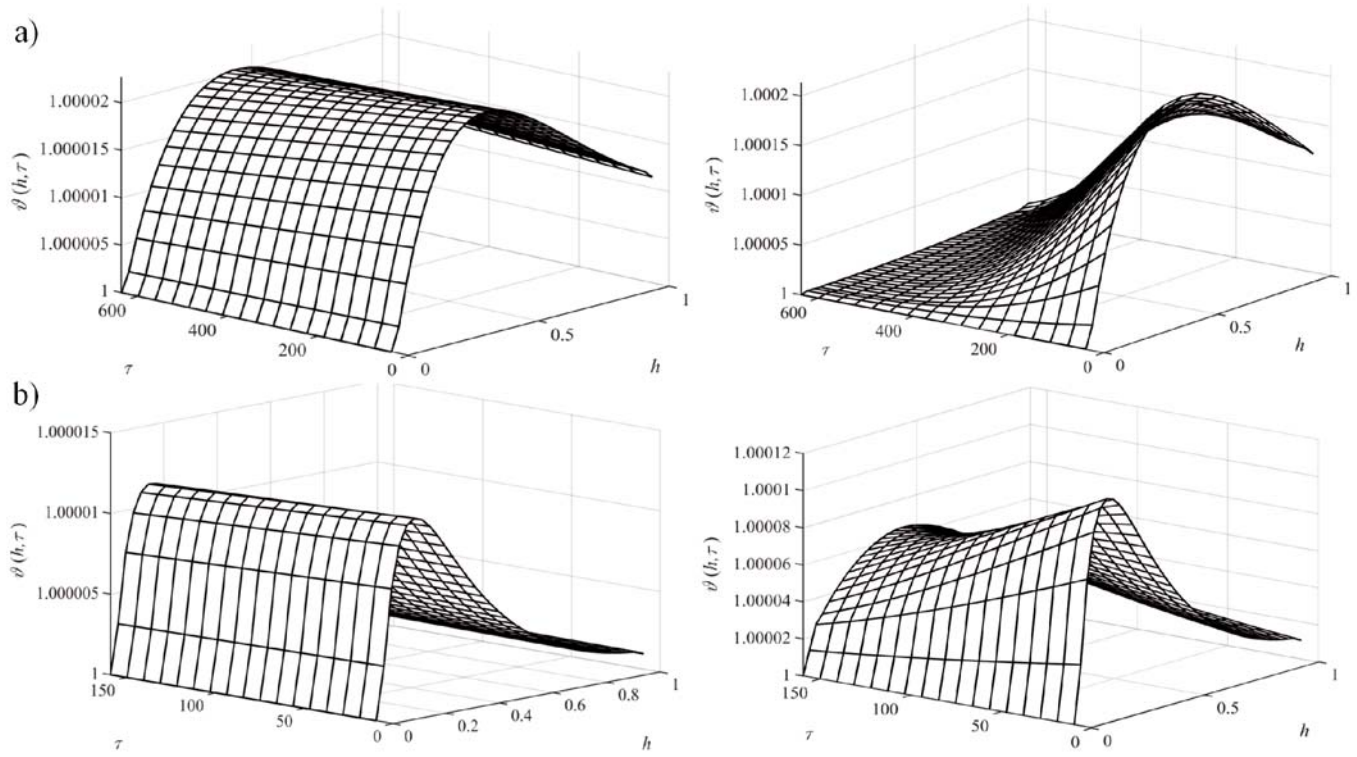

Figure 7. Distribution of the bulk temperature $\vartheta(h,\tau)$ as a function of dimensionless bed length (h) and biocatalyst age (τ) in the HPD process under combined effect of EDR and IDR for OFT of 308 K, feed HP concentration of $C_{S,In} = 1 \cdot 10^{-3}$ kmol $\cdot$ m^{-3} (left) and $C_{S,In} = 1 \cdot 10^{-2}$ kmol $\cdot$ m^{-3} (right), as well as for feed flow rate of: (a) Q =20 $\cdot$ 10^{-8} m^3 $\cdot$ s^{-1}, τ_f = 640, (b) Q = 5 $\cdot$ 10^{-8} m^3 $\cdot$ s^{-1}, τ_f = 160

ters can monotonically decrease (increase) alongside of the reactor length when the feed temperature is higher (lower or in the case of adiabatic process) than that of the jacket fluid temperature.

The time-average HP conversions (α_m) predicted for the feed HP concentration of $C_{S,In} = 5\times10^{-3}$ kmol . m^{-3} and the various jacket temperatures in the HPD process controlled by EDR, as well as combined effect of EDR and IDR have been listed in Table 4.

Table 4. Exemplary values of time-average HP conversion, α_m, and TUC activity obtained for various jacket temperature in the HPD process occurring under EDR, as well as combined effect of EDR and IDR

$Q\times10^8$ m^3 s^{-1}		$\vartheta < 1$		$\vartheta = 1$		$\vartheta > 1$	
		EDR	G	EDR	G	EDR	G
20	α_m	0.946	0.813	0.937	0.811	0.919	0.775
	$\overline{C}_{Em}$	0.470	0.549	0.286	0.380	0.114	0.178
10	α_m	0.984	0.915	0.988	0.928	0.988	0.932
	$\overline{C}_{Em}$	0.731	0.755	0.621	0.642	0.459	0.481
5	α_m	0.995	0.962	0.997	0.972	0.998	0.978
	$\overline{C}_{Em}$	0.865	0.872	0.804	0.808	0.716	0.715

EDR – process under external diffusional resistances, G – process under combined effect of EDR and IDR

It can be said that at the higher values of the heat exchanger temperature and the feed flow rate conversion of HP becomes inefficient.

CONCLUSIONS

The following conclusions can be drawn based on the presented simulation study carried out for parametric values:

– In the hydrogen peroxide decomposition process occurring in a fixed-bed reactor the feed temperature can be indicated, that maximizes the time-averaged HP conversion at the reactor outlet; it is closely related to the feed flow rate, and to diffusional resistances. The more significant diffusional resistances (the lower value of effectiveness factor), the lower the feed HP concentration, and the higher enzyme activity, the higher the temperature is that yields the maximum (or the highest) value of the time-average HP conversion.

– The hydrogen peroxide decomposition is the fastest in the presence of a fresh TUC, and decreases with increasing distance from the reactor inlet as well as when biocatalyst is aging. This is reflected in the decreasing TUC activity, which is the lowest at the highest HP concentration. The lower the feed HP concentration, and the shorter the biocatalyst age, the higher conversion can be achieved.

– The lower the feed flow rate, the higher time-average HP conversion, and at the same time, the higher average TUC activity (higher operational stability) in the bed can be achieved. Thus, with lower, Q, and after utilization time,τ_f, a biocatalyst replacement is recommended only in the initial part of the bioreactor, while at higher feed flow rates biocatalyst replacement along the entire bioreactor length is recommended.

– In biotransformation with parallel deactivation of enzyme the bulk liquid temperature can monotonically increase (decrease) alongside of the bioreactor length when the feed temperature is lower (higher) than the jacket fluid temperature or can achieve a maximum value when the feed temperature is equal to that of the jacket fluid. This maximum is more noticeable at the lower the feed flow rate, and the higher the HP

concentration, while an increase in the feed HP concentration shifts the maximum temperature occurrence towards the shorter biocatalyst age. Thermal effect of the industrial decomposition process of HP makes the temperature rise along the reactor length negligible so the temperature conditions in the reactor can be considered as being isothermal.

– The results of this study not only provide numerical solutions but also a deep understanding of the biotransformation with parallel biocatalyst deactivation. They can be indispensable to scale up the bioreactor for HPD process without the prior estimation of kinetic and process parameters required to select operating conditions for which the productivity of the FXBR under consideration attains the maximum or is the highest.

NOMENCLATURE

a_m – external surface area for mass transfer, $m^2 \cdot m^{-3}$
Bi – Biot number ($= k_{mL} d_P / 6 D_{eff}$)
C_S – bulk substrate concentration, $kmol \cdot m^{-3}$
C_E – enzyme activity, $kg \cdot m^{-3}$
C_P – heat capacity for the bulk liquid, $J \cdot kg^{-1} \cdot K^{-1}$
d_P – particle diameter, m
D_f – substrate diffusivity, $m^2 \cdot s^{-1}$
D_{eff} – effective diffusion coefficient, $m^2 \cdot s^{-1}$
Da – Damköhler number ($=k_R/k_{mL}$)
E_R – activation energy for reaction, $J \cdot mol^{-1}$
E_D – activation energy for deactivation, $J \cdot mol^{-1}$
h – dimensionless distance from reactor inlet ($= z/L$)
H_R – dimensionless heat of reaction ($= (-\Delta H_R) C_{S,In} / \rho C_P T_{In}$)
$(-\Delta H_R)$ – heat of reaction, $J \cdot mol^{-1}$
K_1 – dimensionless number ($= k_R a_m L / U_S$)
K_2 – dimensionless number ($= k_D C_{In} L / U_S$)
k_{mL} – mass transfer coefficient, $m \cdot s^{-1}$
k_D – modified rate constant for deactivation ($=\nu_D/K_D$), $m^3 \cdot kmol^{-1} \cdot s^{-1}$
k_{D0} – pre-exponential factor for deactivation rate constant, $m^3 \cdot kmol^{-1} \cdot s^{-1}$
k'_R – modified rate constant for reaction ($=\nu_R/K_M$), $m^3 \cdot kg^{-1} \cdot s^{-1}$
k_{R0} – pre-exponential factor for enzymatic reaction rate constant, $m^3 \cdot kg^{-1} \cdot s^{-1}$
k_R – modified rate constant for reaction ($= k'_R C_{E0} / a_m$), $m \cdot s^{-1}$
L – bed depth, m
Pe_{mL} – Peclet number for mass transfer ($= U_S L / \varepsilon D_L$)
Pe_{qL} – Peclet number for heat transfer ($= \rho c_P U_S L / \varepsilon \Lambda_x$)
Pr – Prandtl number ($= C_P \eta / \lambda$)
r_m – mass transfer rate, $kmol \cdot m^{-3} \cdot s^{-1}$
r_S – reaction rate, $kmol \cdot m^{-3} \cdot s^{-1}$
St_H – Stanton number ($= 4\alpha_W L / D_R \rho C_P U_S$)
t – biocatalyst utilization time (biocatalyst age) or time, s
T_{In} – feed temperature, K
T_W – heat exchanger temperature, K
U_S – superficial velocity, $m \cdot s^{-1}$
z – distance from reactor inlet, m

Greek letters

α_W – heat transfer coefficient, $W \cdot m^{-2} \cdot K^{-1}$
α_m – time-average substrate conversion at the reactor outlet
β_i – dimensionless Arrhenius number defined as ($= E_i/RT_{In}$) (i = D, R)
ε – porosity of the porous medium (= 0.3)
η – fluid viscosity, $kg \cdot m^{-1} \cdot s^{-1}$
η_{eff} – effectiveness factor
Λ_x – axial heat conduction in liquid phase, $W \cdot m \cdot K^{-1}$
λ – liquid thermal conductance, $W \cdot m \cdot K^{-1}$
ν_D – rate constant for deactivation, s^{-1}
ν_R – rate constant for reaction, $kmol \cdot kg^{-1} \cdot s^{-1}$
ϱ – liquid density, $kg \cdot m^{-3}$
τ – tortuosity factor (Eq. (15)), dimensionless biocatalyst utilization time ($=tU_s/L$)

LITERATURE CITED

1. Maria, G. (2012). Enzymatic reactor selection and derivation of the optimal operation policy, by using a model-based modular simulation platform. Comput. Chem. Eng. 36(0), 325–341. DOI: 10.1016/j.compchemeng.2011.06.006.

2. Maria, G. & Crisan M. (2015). Evaluation of optimal operation alternatives of reactors used for d-glucose oxidation in a bi-enzymatic system with a complex deactivation kinetics. Asia – Pac. J. Chem. Eng. 10(1), 22–44. DOI: 10.1002/apj.1825.

3. Berendsen, W.R., Lapin, A. & Reuss, M. (2007). Non-isothermal lipase-catalyzed kinetic resolution in a packed bed reactor: Modeling, simulation and miniplant studies. Chem. Eng. Sci. 62(9), 2375–2385. DOI: 10.1016/j.ces.2007.01.006.

4. Grubecki, I. (2016). How to run biotransformations—At the optimal temperature control or isothermally? Mathematical assessment. J. Proc. Control 44(0), 79–91. DOI: 10.1016/j.jprocont.2016.05.005.

5. Tükel, S.S., Hürrem, F., Yildirim, D. & Alptekin, Ö. (2013). Preparation of crosslinked enzyme aggregates (CLEA) of catalase and its characterization. J. Mol. Catal. B: Enzym. 97(0), 252–257. DOI: 10.1016/j.molcatb.2013.09.007.

6. Grigoras, A.G. (2017). Catalase immobilization—A review. Biochem. Eng. J. 117, Part B(0), 1–20. DOI: 10.1016/j.bej.2016.10.021.

7. Grubecki, I. (2017). External mass transfer model for hydrogen peroxide decomposition by Terminox Ultra catalase in a packed-bed reactor. Chem. Proc. Eng. 38(2), 307–319. DOI: 10.1515/cpe-2017-0024.

8. Do, D.D. & Weiland, R.H. (1981). Fixed bed reactors with catalyst poisoning: First order kinetics. Chem. Eng. Sci. 36(1), 97–104. DOI: 10.1016/0009-2509(81)80051-6.

9. Do, D.D. & Weiland, R.H. (1981). Enzyme deactivation in fixed bed reactors with michaelis-menten kinetics. Biotechnol. Bioeng. 23(4), 691–705. DOI: 10.1002/bit.260230404.

10. Do, D.D. (1984). Enzyme deactivation studies in a continuous stirred basket reactor. Chem. Eng. J. 28(3), B51-B60. DOI: 10.1016/0300-9467(84)85063-7.

11. Do, D.D. & Weiland, R.H. (1981). Deactivation of single catalyst particles at large Thiele modulus. Travelling wave solutions. Ind. Eng. Chem. Fundam. 20(1), 48–54. DOI: 10.1021/i100001a009.

12. Costa, S.A., Tzanov, T., Filipa Carneiro, A., Paar, A., Gübitz, G.M. & Cavaco-Paulo, A. (2002). Studies of stabilization of native catalase using additives. Enzyme Microb. Technol. 30(3), 387–391. DOI: 10.1016/S0141-0229(01)00505-1.

13. Alptekin, Ö., Seyhan Tükel, S., Yildirim, D. & Alagöz, D. (2011). Covalent immobilization of catalase onto spacer-arm attached modified florisil: Characterization and application to

batch and plug-flow type reactor systems. Enzyme Microb. Technol. 49(6–7), 547–554. DOI: 10.1016/j.enzmictec.2011.09.002.

14. Trusek-Hołownia, A. & Noworyta, A. (2015). Efficient utilisation of hydrogel preparations with encapsulated enzymes – a case study on catalase and hydrogen peroxide degradation. Biotechnol. Rep. 6(0), 13–19. DOI: 10.1016/j.btre.2014.12.012.

15. Ladero, M., Santos, A. & García-Ochoa, F. (2001). Diffusion and chemical reaction rates with nonuniform enzyme distribution: An experimental approach. Biotechnol. Bioeng. 72(4), 458–467. DOI: 10.1002/1097-0290(20000220)72:4<458::AID-BIT1007>3.0.CO;2-R.

16. Ogura, Y. (1955). Catalase activity at high concentration of hydrogen peroxide. Archives of Biochemistry and Biophysics 57(2), 288–300. DOI: 10.1016/0003-9861(55)90291-5.

17. Vasudevan, P.T. & Weiland, R.H. (1990). Deactivation of catalase by hydrogen peroxide. Biotechnol. Bioeng. 36(8), 783–789. DOI: 10.1002/bit.260360805.

18. Sherwood, T.G., Pigford, R.L. & Wilke, C.R. Mass Transfer, in: Clark B.J., Maisel J.W. (Eds.). New York, USA McGraw-Hill Inc.; 1975.

19. Shen, L. & Chen, Z. (2007). Critical review of the impact of tortuosity on diffusion. Chem. Eng. Sci. 62(14), 3748–3755. DOI: 10.1016/j.ces.2007.03.041.

20. Do, D.D. & Hossain, M.M. (1987). A new method to determine active enzyme distribution, effective diffusivity, rate constant for main reaction and rate constant for deactivation. Biotechnol. Bioeng. 29(5), 545–551. DOI: 10.1002/bit.260290502.

21. Martin, A.D. (2000). Interpretation of residence time distribution data. Chem. Eng. Sci. 55(23), 5907–5917. DOI: 10.1016/S0009-2509(00)00108-1.

22. Testu, A., Didierjean, S., Maillet, D., Moyne, C., Metzger, T. & Niass, T. (2007). Thermal dispersion for water or air flow through a bed of glass beads. Int. J. Heat Mass Transfer 50(7–8), 1469–1484. DOI: 10.1016/j.ijheatmasstransfer.2006.09.002.

23. Eissen, M., Zogg, A. & Hungerbühler, K. (2003). The runaway scenario in the assessment of thermal safety: simple experimental access by means of the catalytic decomposition of H_2O_2. J. Loss Prevent. Proc. 16(4), 289–296. DOI: 10.1016/S0950-4230(03)00022-6.

24. Dixon, A.G. & Cresswell, D.L. (1979). Theoretical prediction of effective heat transfer parameters in packed beds. AlChE J. 25(4), 663–676. DOI: 10.1002/aic.690250413.

25. Lin, S.H. (1991). Optimal feed temperature for an immobilized enzyme packed-bed reactor. J. Chem. Technol. Biotechnol. 50(1), 17–26. DOI: 10.1002/jctb.280500104.